

# Evaluation of the Effect of a Step Change in Piezo Actuator Structure on Vibration Reduction Level in Plates

Jerzy WICIAK, Roman TROJANOWSKI

*AGH University of Science and Technology*

Al. A. Mickiewicza 30, 30-059 Kraków, Poland; e-mail: wiciak@agh.edu.pl

*(received November 17, 2014; accepted December 18, 2014)*

This paper presents numerical analyses and a physical experiment on efficiency of different shapes and material composition of piezo actuators on vibration reduction. For this purpose numerical models of a plate clamped on all sides with piezo actuators attached were developed. The elements used were either standard homogeneous elements or the proposed two-part elements with different material composition for inner and outer part of piezo ceramic. Numerical analyses were performed using ANSYS software.

**Keywords:** vibration reduction, two-part elements, different material composition.

## 1. Introduction

For more than 20 years, piezo elements are being used for active methods. Since the works of DIMITRIADIS, FULLER, and ROGERS (1991) these materials have been typically used for beams (BRAŃSKI, 2013; FERDEK, KOZIEŃ, 2013; KOZIEŃ, 2013; AUGUSTYN, KOZIEŃ, 2014) and plate structures (SEKOURI *et al.*, 2004; WICIAK, 2007; 2008; TROJANOWSKI, WICIAK, 2010; BRAŃSKI, SZELA, 2008; 2011; WICIAK, TROJANOWSKI, 2013; 2014b; IWAŃSKI, WICIAK, 2013). Usually one starts with an analytical model (BRAŃSKI, 2013; SEKOURI *et al.*, 2004; WICIAK, TROJANOWSKI, 2013; 2014b; KOZIEŃ, 2013; JABŁOŃSKI, OZGA, 2012), followed by a numerical model (FERDEK, KOZIEŃ, 2013; KOZIEŃ, WICIAK, 2007; WICIAK, 2008; BRAŃSKI, SZELA, 2008; 2011; WICIAK, TROJANOWSKI, 2013; 2014b; IWAŃSKI, WICIAK, 2013; AUGUSTYN, KOZIEŃ, 2014) possibly verified by a physical experiment (WICIAK, 2007; 2008; TROJANOWSKI, WICIAK, 2010; IWAŃSKI, WICIAK, 2013; JABŁOŃSKI, OZGA, 2012). In most cases, a significant reduction of vibration or/and acoustic pressure can be achieved. A special case of piezoelectric materials are Functionally Graded Materials – FGMs (FERDEK, KOZIEŃ, 2013; PIETRZAKOWSKI, 2007; LOY *et al.*, 1999). Gradient materials are composite materials prepared by combining and mixing two or more different component materials arranged along the thickness in accordance with the law of the volume fraction.

This paper focuses on a specific type of piezo elements, hereinafter referred to as two-part elements. Such elements consist of an inner part and an outer part, both having different material compositions.

Previous publications of the authors that led to this paper started with mathematical aspects and numerical modelling of a thin circular plate homogeneous piezo elements attached (WICIAK, TROJANOWSKI, 2013). After that there was a paper (WICIAK, TROJANOWSKI, 2014a) that presented the results of numerical analyses of vibration reduction and voltage efficiency of square- and disc-based piezo actuators with homogeneous and two-part material composition (some of these results will be also used in this paper). There is also a mathematical and numerical study of the effect of different placement of the inner part of a two-part element on its work (WICIAK, TROJANOWSKI, 2014a).

This paper will show results for two groups of numerical models and a physical experiment. The first group consists of general models of a steel plate clamped on all sides with two piezo elements attached. One of them is always a homogeneous element used for plate excitation. The other one is used for vibration reduction and depending on the case it can have a different shape and material composition. It can be a square-, disc-, or triangle-based element of either homogeneous or two-part composition.

The second group is actually one model that was made to resemble the physical experiment. Therefore

its geometry and arrangement of piezo elements are the same as for the experiment. There are 7 piezo elements attached in total: one is used for plate excitation, two pairs of actuators, and two sensors. The actuators are rectangle-based elements with either homogeneous or two-part composition. All other piezo elements are homogeneous square-based elements.

## 2. Numerical models

### 2.1. General models

General models represented a steel plate ( $500 \times 500 \times 2$  mm) clamped on all sides with two piezo elements attached. One of these piezo elements was always a homogeneous element with a square as a base, the base area of  $1600 \text{ mm}^2$ , height of 1 mm, and material properties of PZ 28. This element was used to excite plate vibrations. The other element had a different shape depending on the model. It could be a square-, disc-, or right-angled triangle-based element. Each model had two possible variants of actuator depending on material composition. These were:

- a homogeneous element with the base area of  $1600 \text{ mm}^2$ , height of 1 mm, and material properties of either PZ 28 or PZ 29 (Fig. 2a, 2c, and 2e);
- a two-part element with the base area of  $1600 \text{ mm}^2$ , height of 1 mm, and material properties of PZ 28 and PZ 29 (either the inner part made of PZ 28 and the outer part of PZ 29, or the inner part made of PZ 29 and the outer part of PZ 28) and the area of the inner part being  $1/4$  of the area of the whole part (Fig. 2b, 2d, and 2f).

Figure 1 shows the modelled plate and arrangement of the piezo elements.

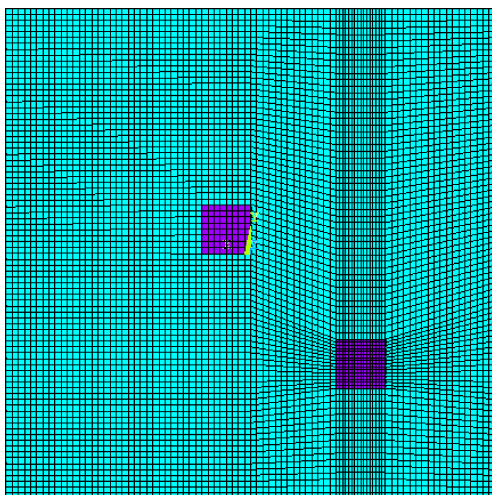


Fig. 1. The modelled plate and arrangement of the piezo elements: near the centre the element is used for plate excitation; the one closer to the edges was used for vibration reduction.

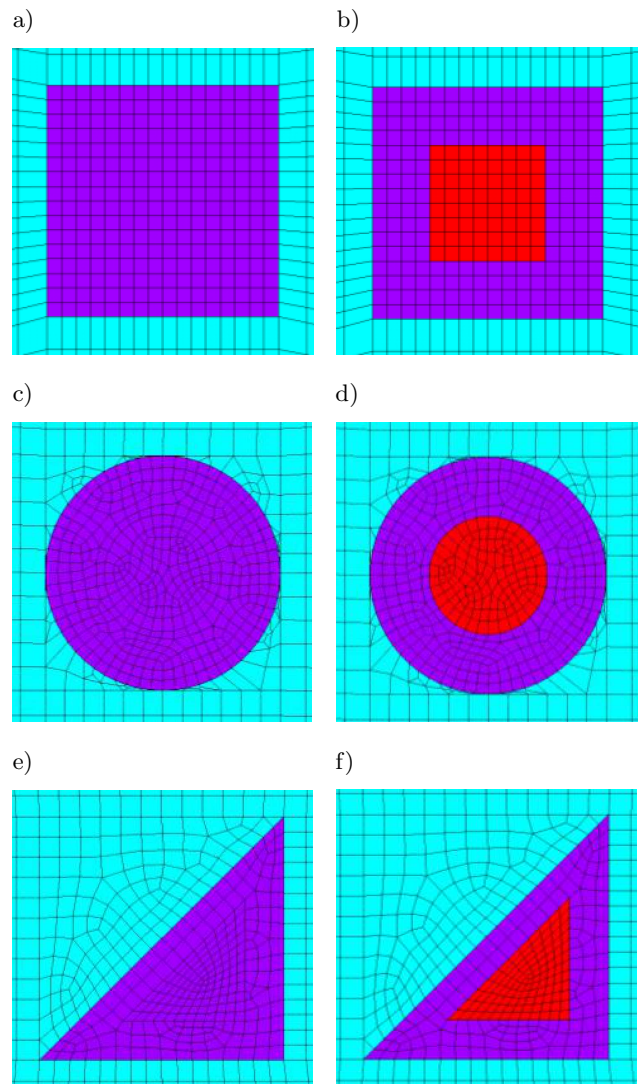


Fig. 2. Modelled piezo elements: a) homogeneous square-based; b) two-part square-based; c) homogeneous disc-based; d) two-part disc-based; e) homogeneous right-angled triangle-based; f) two-part right-angled triangle-based.

Table 1 shows which elements were used when developing the models together with material properties that were assigned to them.

Table 1. Parameters of models.

Structural elements	Element used for modelling	Material properties
Plate	SOLSH190	$E = 1.93 \cdot 10^{11} \text{ Pa}$ , $\nu = 0.29$ $\rho = 7800 \text{ kg/m}^3$
Piezo element used for plates excitation	SOLID226	Properties of PZ 28
Actuators	SOLID226	Combination of properties of PZ 28 and PZ 29

Modal analyses were performed to find the first six modes after which modes 1 and 5 were selected for further analyses (mode 1 was chosen because it is the most basic of the modes and mode 5 because the placement of elements is near its anti-nodes). For harmonic analyses, a voltage of 100 V was applied to the element responsible for plate excitation. The search for optimal amplitudes and phases of voltage for actuators was done using internal ANSYS optimisation procedures. The goal function was assumed in the form:

$$J = \min \sum_{i=1}^n |\mathbf{X}_{\text{sum}}(i)|, \quad (1)$$

where min is the smallest value of sum;  $\mathbf{X}_{\text{sum}}(i)$  is the displacement vector in  $i$ -th node;  $n$  is the number of nodes (in this case all nodes making up the area of the plate: 7654 nodes with square-based elements, 7296 nodes with disc-based elements and 6932 nodes with triangle-based elements).

It has been readily determined that the optimal phase for the first mode would be  $180^\circ$  and  $0^\circ$  for the fifth mode. This allowed to reduce the number of design variables to 1 – the amplitude of the voltage applied to the actuator. The number of steps performed during one optimisation procedure was chosen to be 30. After each completion of the procedure it was repeated with the amplitude range being narrowed. In the final run the range was 5 V.

A detailed explanation on the square- and disc-based elements and results were shown in paper WICIAK, TROJANOWSKI (2014a).

### 2.2. Advanced model

An advanced model was created with the aim to closely represent the physical experiment. Therefore the geometry of the plate, piezo elements, as well as elements types and their arrangement were the same as in the experiment (Figs. 3 and 4). The material of the plate was the same as for one of the plates used in

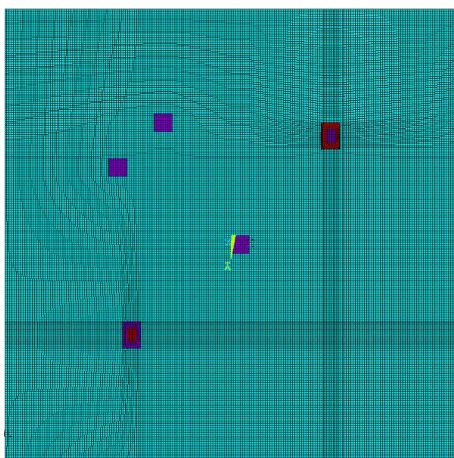


Fig. 3. Modelled plate.

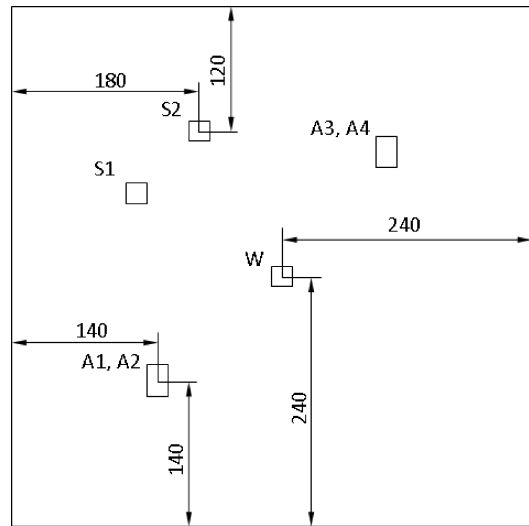


Fig. 4. Arrangement of piezo elements placement: W – excitation, A1-A4 – actuators, S1-S2 – sensors.

experiment. The material used for piezo elements was the same as for the last model (due to unavailability of sufficiently precise data on materials used for piezo actuators in the experiment).

The element labelled as W was used for excitation and was a square-based homogeneous element with  $a = 20$  mm,  $h = 1$  mm, and material properties of PZ 28. Elements S1 and S2 were used as sensors with dimensions and material properties same as for W. A1-A4 were rectangle-based  $30 \times 20 \times 1$  mm elements used as actuators with either homogeneous or two-part composition. Their material composition was either PZ 28 or PZ 29 (homogeneous case) or a composition of the two (two-part case). Again, the inner part area was 1/4 of the whole base area. Actuators were paired, meaning that A1 and A2 were placed in the same spot but on different sides of the plate and had the same composition. The same was true for A3 and A4. Possible variations of the model were:

- homogeneous actuators with A1 and A2 being made of PZ 28, and A3 and A4 of PZ 29;
- two-part actuators with A1 and A2 made of PZ 28/PZ 29 (inner/outer part) and A3 and A4 made of PZ 29/PZ 28.

Table 2 shows model parameters for the advanced model.

As with the previous models, modal analysis was performed to find the first six mode shapes and two of them were used in further analyses (the first and fourth). The first mode was chosen for the same reason as for the previous models. The fourth mode was chosen over the fifth one because in the physical experiment it should require less energy (lower voltage applied to actuators) to reduce it. The harmonic analyses and optimisation procedure settings were the same as for previous models, except for the fact that they

Table 2. Parameters of models.

Structural elements	Element used for modelling	Material properties
Plate	SOLSH190	$E = 2.2 \cdot 10^{11}$ Pa, $\nu = 0.3$ $\rho = 7700$ kg/m <sup>3</sup>
Piezo element used for plates excitation and sensors	SOLID226	Properties of PZ 28
Actuators	SOLID226	Properties of either PZ 28 or PZ 29, or combination of booth

were carried out for two goal functions. The first goal function used was the same as for the previous models (Eq. (1)) with  $n = 42884$  nodes. The second goal function used was

$$J_2 = \min(V_k), \quad (2)$$

where  $V_k$  is the amplitude of voltage on  $k$ -th sensor ( $k = 1$  or  $2$ ) and min means the smallest value found. The obtained results are presented in Sec. 4 below in comparison with the experimental ones.

### 3. Physical experiment

The subjects of the experiment were two plates ( $500 \times 500 \times 2$  mm) clamped on all sides with piezo elements attached to them. One of them was made from steel, the other one was from aluminium. For both plates, the number, arrangement, and function of piezo elements were the same. The arrangement of piezo elements is presented in Fig. 4. Figure 5 shows the front and back of the steel plate mounted in the laboratory stand.

The dimensions of elements W, S1, and S2 are the same as in the advanced model ( $20 \times 20 \times 1$  mm) and were made of PZT 4D. The actuators were 1 mm thicker than in the experiment ( $30 \times 20 \times 2$  mm) and their material composition was as follows:

- homogeneous elements made of PZ 45 (A1 and A2) or PZ 54 (A3 and A4) were attached to the steel plate;
- two-part elements with the inner part having 1/4 area size of the whole element, where for A1 and A2 the inner part was made from PZ 45 and the outer one of PZ 54, A3 and A4 had the inner part made from PZ 54 and the outer one of PZ 45.

The measuring equipment consisted of a PC computer with the National Instruments LabVIEW software installed, an NI 9215 module being used to the read sensor data, as well as an NI PCI 6733 and voltage amplifier used for the output signals. Resonance

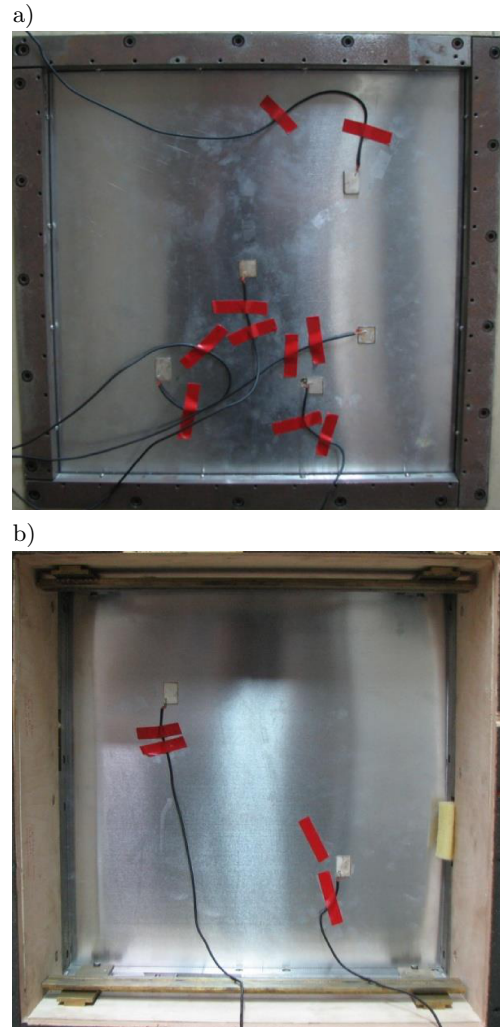


Fig. 5. Front (a) and back (b) of the steel plate in the laboratory stand.

frequencies were obtained using the swept sine signal. From the frequencies determined for each plate four were chosen for which readings from both sensors were comparable. During the experiment, the plate was excited by a sine signal with a given resonance frequency and with the amplitude of 25 V for the steel plate and 5 V for the aluminium one. Reduction was carried out using each actuator one at a time, first on Sensor 1 (S1) and then on Sensor 2 (S2). The goal function used was given by Eq. (2). The upper limit of voltage applied to actuators was 350 V. Vibration reduction was optimised by means of manually searching for the optimal phase and amplitude of voltage applied to a given actuator with minimum steps being 5 V and  $1^\circ$ .

### 4. Results

The obtained reduction ( $L_{\text{red}}$ ) was calculated differently depending on the fact whether the goal function  $J_1$  or  $J_2$  was used. With  $J_1$  (Tables 3 and 4) it was calculated as:

$$L_{\text{red}} = 20 \log \frac{\sum_{i=1}^n |\mathbf{X}_{1\text{sum}}(i)|}{\sum_{i=1}^n |\mathbf{X}_{2\text{sum}}(i)|}, \quad (3)$$

where  $\mathbf{X}_{1\text{sum}}(i)$  is the displacement vector in  $i$ -th node before the reduction,  $\mathbf{X}_{2\text{sum}}(i)$  is the displacement vector in  $i$ -th node after the reduction, and  $n$  is the number of nodes making the area of the plate (same as for Eq. (1)).

Table 3a. Results for the square-based piezo actuators.

Material inner/outer	Mode	U [V]	$\varphi$ [°]	$L_{\text{red}}$ [dB]
PZ 28	1	365.29	180.00	41.3
PZ 29/PZ 28	1	294.88	180.00	41.3
PZ 29	1	198.29	180.00	41.0
PZ 28/PZ 29	1	228.29	180.00	41.3
PZ 28	5	159.95	360.00	34.7
PZ 29/PZ 28	5	129.10	360.00	35.0
PZ 29	5	86.93	360.00	34.6
PZ 28/PZ 29	5	100.45	360.00	34.4

Table 3b. Results for the disc-based piezo actuators.

Material inner/outer	Mode	U [V]	$\varphi$ [°]	$L_{\text{red}}$ [dB]
PZ 28	1	371.94	180.00	39.9
PZ 29/PZ 28	1	300.24	180.00	39.8
PZ 29	1	200.24	180.00	39.8
PZ 28/PZ 29	1	230.81	180.00	39.9
PZ 28	5	161.98	360.00	35.1
PZ 29/PZ 28	5	131.24	360.00	34.8
PZ 29	5	87.29	360.00	35.2
PZ 28/PZ 29	5	101.24	360.00	35.3

Table 3c. Results for the right-angled triangle-based piezo actuators.

Material inner/outer	Mode	U [V]	$\varphi$ [°]	$L_{\text{red}}$ [dB]
PZ 28	1	255.02	180.00	43.6
PZ 29/PZ 28	1	212.02	180.00	42.9
PZ 29	1	145.55	180.00	43.3
PZ 28/PZ 29	1	165.55	180.00	43.2
PZ 28	5	201.24	360.00	35.5
PZ 29/PZ 28	5	156.94	360.00	35.0
PZ 29	5	109.24	360.00	35.0
PZ 28/PZ 29	5	127.69	360.00	35.5

Description for Tables 3a, 3b, and 3c: material – the material used for the inner/outer part of the actuator; mode – the mode shape; U – the amplitude of voltage applied to the element;  $\varphi$  – the phase angle of the voltage applied to the element;  $L_{\text{red}}$  – the vibration reduction level obtained from the simulation calculated from Eq. (3).

Table 4. Results of the numerical analyses concerning plate vibration reduction with  $J_1$  criterion:  $f$  – the frequency,  $A_i$  – the element used as actuator, mat. comp. – the material composition of the inner and outer part of the actuator,  $U_i$  – the amplitude of voltage applied to the actuator,  $L_{\text{red}}$  – the reduction level calculated from Eq. (3).

Mode	$A_i$	Mat. comp. (inner/outer)	$U_i$ [V]	$L_{\text{red}}$ [dB]
1	A1	PZ 29/PZ 28	257.29	46.8
		PZ 28/PZ 28	318.24	46.8
	A2	PZ 29/PZ 28	234.29	46.7
		PZ 28/PZ 28	284.55	46.5
	A3	PZ 28/PZ 29	200.17	46.6
		PZ 29/PZ 29	173.81	46.5
A4	PZ 28/PZ 29	173.55	46.4	
	PZ 29/PZ 29	152.98	46.7	
4	A1	PZ 29/PZ 28	2.77	15.1
		PZ 28/PZ 28	3.38	15.1
	A2	PZ 29/PZ 28	2.45	14.9
		PZ 28/PZ 28	3.00	15.0
	A3	PZ 28/PZ 29	2.14	15.1
		PZ 29/PZ 29	1.85	15.0
	A4	PZ 28/PZ 29	1.87	14.9
		PZ 29/PZ 29	1.61	14.8

With  $J_2$  (Tables 5–8)  $L_{\text{red}}$  was calculated as:

$$L_{\text{red}} = 20 \log \frac{V_{1k}}{V_{2k}}, \quad (4)$$

where  $V_{1k}$  is the amplitude of voltage on sensor before reduction and  $V_{2k}$  is the amplitude of voltage on sensor after reduction.

Results of numerical simulations when using the goal function  $J_1$  (reduction of vibration using the whole area of the plate – Tables 3–4) show no significant differences between vibration reduction obtained using elements with a different composition. In most cases, differences are less than 1 dB and independent of both actuator shape and mode shape (Figs. 6–8).

There were some differences between different shapes of actuators modelled. The one between the square- and disc-based elements was about 1.5 dB depending on the mode, but the difference between a triangle-based actuators was up to about 3 dB for the first mode and as high as nearly 9 dB for the fifth mode.

The voltage applied to the actuators followed a simple rule – the greater the share of a material with “stronger” piezo ceramic constants, the lower the amplitude.

As it was already mentioned above, results for advanced model with the goal function  $J_1$  (Table 4) did not show any significant differences when using a different material composition. This changed when

Table 5. Results of the numerical analyses concerning plate vibration reduction with  $J_2$  criterion (for S1):  $f$  – the frequency,  $A_i$  – the element used as actuator, mat. comp. – the material composition of the inner and outer part of the actuator,  $U_i$  – the amplitude of voltage applied to the actuator,  $L_{\text{red}}$  – the reduction level calculated from Eq. (4).

Mode	$A_i$	Mat. comp. (inner/outer)	$U_i$ [V]	$L_{\text{red}}$ [dB]
1	A1	PZ 29/PZ 28	257.31	47.8
		PZ 28/PZ 28	318.87	47.5
	A2	PZ 29/PZ 28	233.98	55.4
		PZ 28/PZ 28	285.24	54.1
	A3	PZ 28/PZ 29	200.29	50.9
		PZ 29/PZ 29	173.29	48.5
	A4	PZ 28/PZ 29	173.81	61.2
		PZ 29/PZ 29	153.09	62.1
4	A1	PZ 29/PZ 28	2.83	20.2
		PZ 28/PZ 28	3.46	20.1
	A2	PZ 29/PZ 28	2.52	20.0
		PZ 28/PZ 28	3.09	20.2
	A3	PZ 28/PZ 29	2.23	20.0
		PZ 29/PZ 29	1.96	19.9
	A4	PZ 28/PZ 29	1.96	20.1
		PZ 29/PZ 29	1.74	20.0

Table 6. Results of the numerical analyses concerning plate vibration reduction with  $J_2$  criterion (for S2):  $f$  – the frequency,  $A_i$  – the element used as actuator, mat. comp. – the material composition of the inner and outer part of the actuator,  $U_i$  – the amplitude of voltage applied to the actuator,  $L_{\text{red}}$  – the reduction level calculated from Eq. (4).

Mode	$A_i$	Mat. comp. (inner/outer)	$U_i$ [V]	$L_{\text{red}}$ [dB]
1	A1	PZ 29/PZ 28	257.29	45.2
		PZ 28/PZ 28	318.24	45.0
	A2	PZ 29/PZ 28	234.29	54.1
		PZ 28/PZ 28	284.94	53.0
	A3	PZ 28/PZ 29	200.24	51.6
		PZ 29/PZ 29	173.81	51.6
	A4	PZ 28/PZ 29	173.81	62.1
		PZ 29/PZ 29	153.09	63.3
4	A1	PZ 29/PZ 28	2.83	19.9
		PZ 28/PZ 28	3.50	19.9
	A2	PZ 29/PZ 28	2.57	19.9
		PZ 28/PZ 28	3.11	19.9
	A3	PZ 28/PZ 29	2.19	20.0
		PZ 29/PZ 29	1.96	20.1
	A4	PZ 28/PZ 29	1.92	20.2
		PZ 29/PZ 29	1.75	20.2

Table 7. Results of the physical experiment for Sensor 1 and the steel plate:  $f$  – the frequency,  $U_i$  – the voltage amplitude applied to  $i$ -th actuator,  $\varphi_i$  – the phase angle of voltage applied to  $i$ -th actuator,  $L_{\text{red S1}}$  – the reduction level calculated from Eq. (4).

$f$ [Hz]	$U_1$ [V]	$\varphi_1$ [°]	$U_2$ [V]	$\varphi_2$ [°]	$U_3$ [V]	$\varphi_3$ [°]	$U_4$ [V]	$\varphi_4$ [°]	$L_{\text{red S1}}$ [dB]
130	45	310	0	0	0	0	0	0	23
130	0	0	40	314	0	0	0	0	23
130	0	0	0	0	55	318	0	0	26
130	0	0	0	0	0	0	45	313	31
230	130	238	0	0	0	0	0	0	34
230	0	0	125	260	0	0	0	0	29
230	0	0	0	0	165	267	0	0	34
230	0	0	0	0	0	0	130	265	34
370	175	263	0	0	0	0	0	0	27
370	0	0	160	261	0	0	0	0	24
370	0	0	0	0	190	271	0	0	31
370	0	0	0	0	0	0	160	261	31
620	225	137	0	0	0	0	0	0	17
620	0	0	215	133	0	0	0	0	20
620	0	0	0	0	270	133	0	0	23
620	0	0	0	0	0	0	210	133	26

Table 8. Results of the physical experiment for Sensor 1 and the aluminium plate:  $f$  – the frequency,  $U_i$  – the voltage amplitude applied to  $i$ -th actuator,  $\varphi_i$  – the phase angle of voltage applied to  $i$ -th actuator,  $L_{\text{red S1}}$  – the reduction level calculated from Eq. (4).

$f$ [Hz]	$U_1$ [V]	$\varphi_1$ [°]	$U_2$ [V]	$\varphi_2$ [°]	$U_3$ [V]	$\varphi_3$ [°]	$U_4$ [V]	$\varphi_4$ [°]	$L_{\text{red S1}}$ [dB]
140	345	44	0	0	0	0	0	0	2
140	0	0	345	10	0	0	0	0	4
140	0	0	0	0	345	47	0	0	13
140	0	0	0	0	0	0	45	43	22
250	345	314	0	0	0	0	0	0	1
250	0	0	345	0	0	0	0	0	3
250	0	0	0	0	335	310	0	0	12
250	0	0	0	0	0	0	35	325	20
430	345	0	0	0	0	0	0	0	2
430	0	0	345	0	0	0	0	0	2
430	0	0	0	0	175	198	0	0	11
430	0	0	0	0	0	0	45	227	13
590	345	0	0	0	0	0	0	0	1
590	0	0	345	0	0	0	0	0	3
590	0	0	0	0	345	348	0	0	4
590	0	0	0	0	0	0	200	276	9

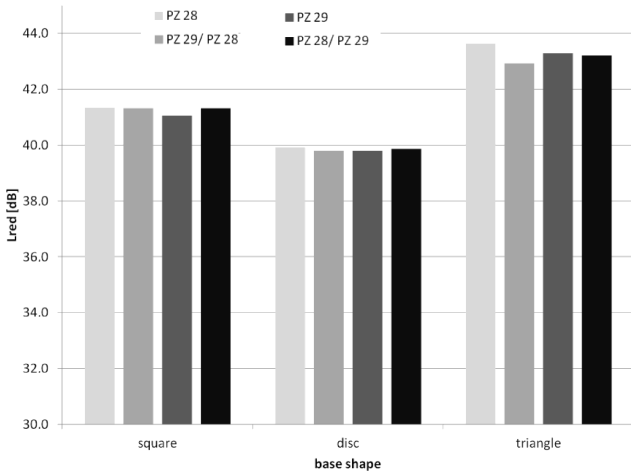


Fig. 6. Reduction obtained for the first mode.

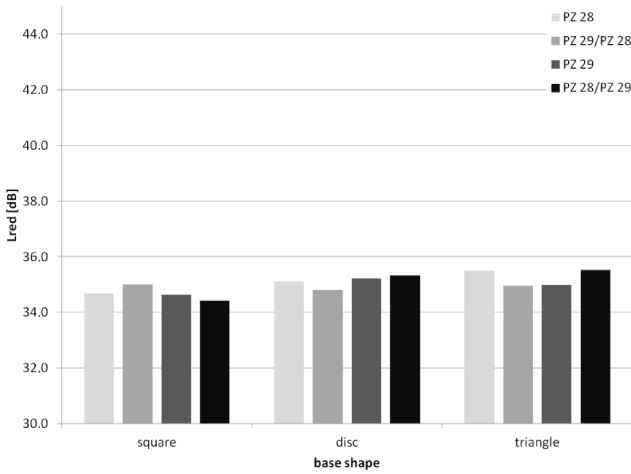


Fig. 7. Reduction obtained for the fifth mode.

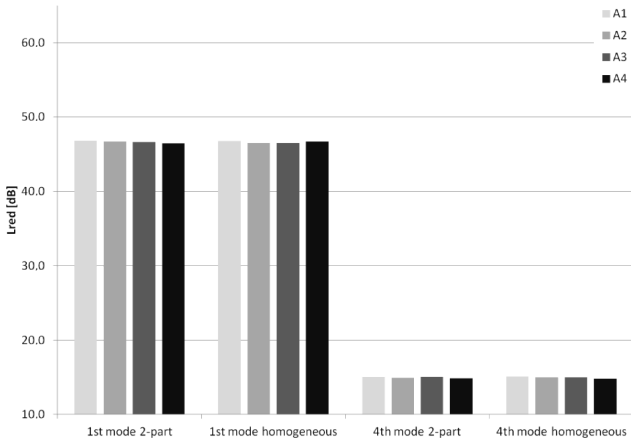


Fig. 8. Reduction obtained for the advanced model with the goal function  $J_1$ .

the calculations were repeated using the goal function  $J_2$  (vibration reduction using a single sensor – Tables 5 and 6). For the first mode, differences in the obtained reduction could be observed ranging from about 7 dB to more than 10 dB. Interestingly, these differences appeared only for the first mode and between the

reductions obtained with the elements A1 and A3 or A2 and A4. Therefore it is possible that these differences result from the finite elements mesh not being exactly symmetrical (although if that were the case it should show for the other mode to). Moreover, this does not explain the differences between the results obtained for A1 and A2, or A3 and A4. These pairs were placed in the same location, but on the opposite sides of the plates.

As far as the applied voltage is considered we can see that when using actuators placed on the opposite side of the plate (as compared to the one used for excitation), the amplitude needed for the same effect is about 10% higher.

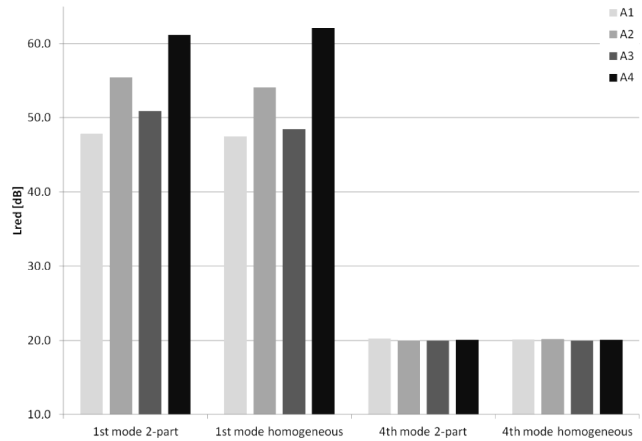


Fig. 9. Reduction obtained for the advanced model with the goal function  $J_2$  (Sensor 1).

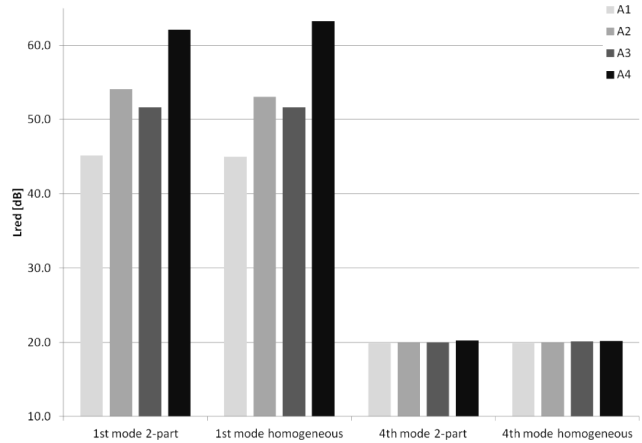


Fig. 10. Reduction obtained for the advanced model with the goal function  $J_2$  (Sensor 2).

The results of the physical experiments are inconclusive. The reductions obtained for the steel plate (the one with homogeneous actuators) vary (Table 7). For some frequencies it was possible to obtain similar reduction levels, while for other one the differences exceed 6 dB (Figs. 11 and 12). It should be noted that all rectangle-shaped piezo elements were especially made for this experiment. The ones attached to the plates

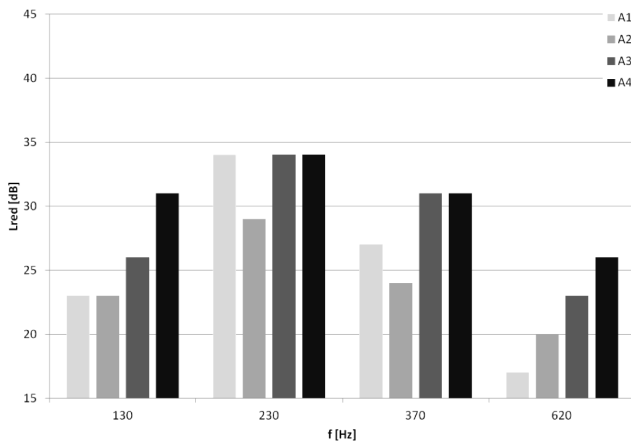


Fig. 11. Reduction obtained for the steel plate with the goal function  $J_2$  (Sensor 1).

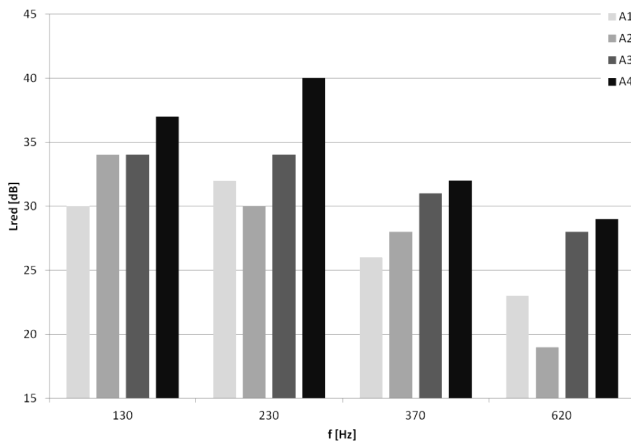


Fig. 12. Reduction obtained for the steel plate with the goal function  $J_2$  (Sensor 2).

were the best samples, from a batch, but unfortunately the samples themselves were not sufficiently repeatable.

Results for the two-part elements (aluminium plate) show that only one actuator was working correctly — A4 (Fig. 13 and 14). Excitation of other ele-

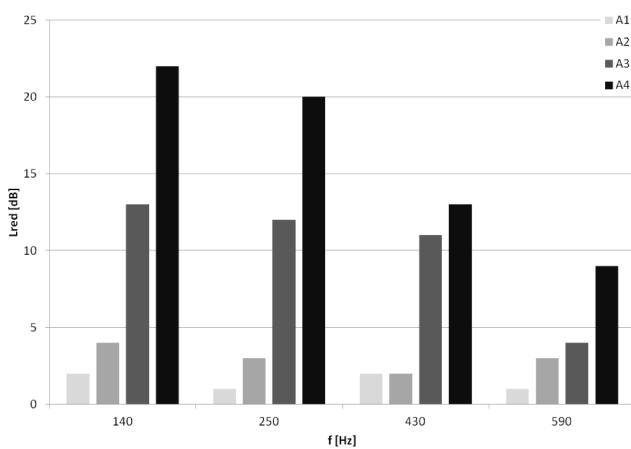


Fig. 13. Reduction obtained for the aluminium plate with the goal function  $J_2$  (Sensor 1).

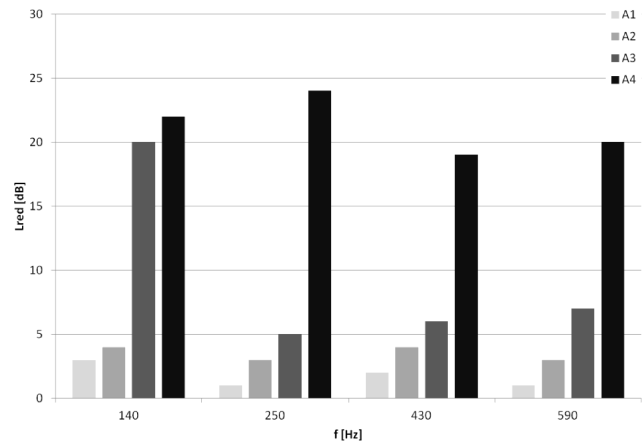


Fig. 14. Reduction obtained for the aluminium plate with the goal function  $J_2$  (sensor 2).

ments resulted basically in no reduction even with the applied voltage nearing the maximum level (Table 8). This suggests that the production process was even worse for two-part elements.

## 5. Conclusions

There were very small differences (less than 1 dB) between the two-part and homogeneous piezo elements when the  $J_1$  goal function was used. With the  $J_2$  criterion for the numerical analyses, there were cases for which differences were as high as 10 dB for specific arrangements of the elements.

There were small differences between different shapes of elements. The difference between the square-based and circle-based elements was about  $\pm 1$  dB depending on the mode shape. For the triangle-based elements and the first mode, the results were about 3 dB better than for disc shape, but for the fifth mode they were up to 9 dB lower.

During the physical experiment it turned out that some of the actuators were not working correctly. Therefore it is difficult to compare the numerical and experimental results. For this reason, the physical experiment should be repeated after improving the production process and with the use of a larger number of samples.

Possible future continuation of this study could involve electric isolation of the inner and outer part of the elements and either using the inner part as a sensor, or controlling both parts independently.

## References

1. AUGUSTYN E., KOZIEŃ M.S. (2014), *A Study on Possibility to Apply Piezoelectric Actuators for Active Reduction of Torsional Beams Vibrations*, Acta Phys. Pol. A, **125**, 4A, A164–A168.



2. BRAŃSKI A., SZELA S. (2008), *Improvement of Effectiveness in Active Triangular Plate Vibration Reduction*, Archives of Acoustics, **33**, 4, 521–530.
3. BRAŃSKI A., SZELA S. (2011), *Evaluation of the Active Plate Vibration Reduction by the Parameter of the Acoustic Field*, Acta Phys. Pol. A, **119**, 6a, 942–945.
4. BRAŃSKI A. (2013), *Effectiveness Analysis of the Beam Modes Active Vibration Protection with Different Number of Actuators*, Acta Phys. Pol. A, **123**, 6, 1123–1127.
5. DIMITRIADIS E.K., FULLER C.R., ROGERS C.A. (1991), *Piezoelectric Actuators for Distributed Vibration Excitation of Thin Plates*, Journal of Vibration and Acoustics, **113**, 1, 100–107.
6. FERDEK U., KOZIEŃ M.S. (2013), *Simulation of Application of FGM Piezoelectric Actuators for Active Reduction of Beam Vibrations*, Acta Phys. Pol. A, **123**, 6, 1044–1047.
7. IWAŃSKI D., WICIAK J. (2013), *Reduction of Vibration of Fluid Loaded Plate with Piezoelectric Elements – a Comparison of Analytical, FEM Harmonic Analysis, and Real Results*, Acta Phys. Pol. A, **123**, 6, 1040–1043.
8. JABLOŃSKI M., OZGA A. (2012), *Determining the Distribution of Values of Stochastic Impulses Acting on a Discrete System in Relation to Their Intensity*, Acta Phys. Pol. A, **121**, 1A, A174–A178.
9. KOZIEŃ M.S. (2013), *Analytical Solutions of Excited Vibrations of a Beam with Application of Distribution*, Acta Phys. Pol. A, **123**, 6, 1029–1033.
10. KOZIEŃ M.S., WICIAK J. (2008), *Reduction of Structural Noise Inside Crane Cage by Piezoelectric Actuators – FEM Simulation*, Archives of Acoustics, **33**, 4, 643–652.
11. LOY C.T, LAM K.Y, REDDY J.N. (1999), *Vibration of Functionally Graded Cylindrical Shells*, International Journal of Mechanical Sciences, **41**, 3, 309–324.
12. PIETRZAKOWSKI M. (2007), *Vibration Control of Functionally Graded Piezoelectric Plates*, Mechanics, **26**, 4, 181–186.
13. SEKOURI E.M. HU Y, NGO A.D. (2004), *Modeling of a circular plate with piezoelectric actuators*, Mechatronics, **14**, 9, 1007–1020.
14. TROJANOWSKI R., WICIAK J. (2010), *Preliminary Results of Laboratory Tested System for Active Control of Plates VIA LabVIEW and Piezoelectric Elements*, Acta Phys. Pol. A, **118**, 1, 168–171.
15. WICIAK J. (2007), *Modelling of Vibration and Noise Control of a Submerged Circular Plate*, Archives of Acoustics, **32**, 4, 265–270.
16. WICIAK J. (2008), *Sound Radiation by Set of L-Jointed Plates With Four Pairs of Piezoelectric Elements*, European Physical Journal-Special Topics, **154**, 229–233.
17. WICIAK M., TROJANOWSKI R. (2013), *Modeling of a Circular Plate with Piezoelectric Actuators of Arbitrary Shape*, Acta Phys. Pol. A, **123**, 6, 1048–1053.
18. WICIAK J., TROJANOWSKI R. (2014a), *The Effect of Material Composition of Piezoelectric Elements with Chosen Shapes on Plate Vibration Reduction*, Acta Phys. Pol. A, **125**, 4a, A179–A182.
19. WICIAK M., TROJANOWSKI R. (2014b), *Numerical Analysis of the Effectiveness of Two-part Piezoactuators in Vibration Reduction of Plates*, Acta Phys. Pol. A, **125**, 4A, A183–A189.